energies

Article

Vibration Model of a Power Capacitor Core under Various Harmonic Electrical Excitations

Jinyu Li *, Xiaoyan Lei, Zhongqiu Zuo and Yi Xiong

China Electric Power Research Institute, Beijing 100192, China; leixiaoyan@epri.sgcc.com.cn (X.L.); zuozhongqiu@epri.sgcc.com.cn (Z.Z.); xiongyi@epri.sgcc.com.cn (Y.X.)
* Correspondence: ljyxjtu@sina.com

Abstract: Power capacitors are widely used in power transmission systems. During their operation, an electric force acting on the electrodes of the power capacitors actuates mechanical vibrations and radiates an audible noise. Considering a power capacitor as a general system, the frequency response with the electric force as the input and mechanical vibration as the output have been measured by engineers in recent years and used to evaluate the acoustic and mechanical features of products. Accidentally, it was found that the frequency of the capacitor vibration was not consistent with its excitation due to electro-mechanical coupling. This electro-mechanical coupling had not been considered in previous vibration models of power capacitors. Therefore, a new vibration model of power capacitors was built up in this paper and a so-called multi-frequency vibration characteristic was revealed. A theoretical analysis showed that the electric force and mechanical vibration of the power capacitors were coupled, which resulted in the multi-frequency vibration. The vibration frequency response was measured and the result was consistent with the vibration model proposed in this paper. Once the frequency of the electric force was near half the natural frequency of the power capacitor, a predominant multi-frequency vibration was triggered and the power capacitor was in a superharmonic resonance.

Keywords: power capacitor; mechanical vibration; electro-mechanical coupling; superharmonic resonance

Citation: Li, J.; Lei, X.; Zuo, Z.; Xiong, Y. Vibration Model of a Power Capacitor Core under Various Harmonic Electrical Excitations. *Energies* **2022**, *15*, 1848. https://doi.org/10.3390/en15051848

Academic Editors: Qiuqin Sun and Tek Tjing Lie

Received: 7 January 2022
Accepted: 1 March 2022
Published: 2 March 2022

1. Introduction

The audible noise of power capacitors originates from mechanical vibration, which is excited by an alternating electric force inside the capacitor cores [1–3]. Due to the negative effects of audible noise, its assessment and mitigation have been taken seriously in power transmission systems [4,5]. Mechanical vibration, as the acoustic source of a power capacitor, needs to be understood first; for example, its generating mechanism and frequency response under the excitation of different electric forces. Therefore, it was deemed significant to build a vibration model of a power capacitor core under various electrical excitations.

Electric forces, as the excitation of mechanical vibration, cannot be directly measured from a power capacitor so most researchers have utilized the square of the voltage on a capacitor to characterize the electrical forces [6–9] based on the relation between the electric force F_e and the terminal voltage $u(t)$, as shown in Equation (1):

$$F_e = \frac{1}{2}\frac{\mathrm{d}C_0}{\mathrm{d}L}u^2(t) = \alpha u^2(t) \tag{1}$$

where F_e is the electric force acting on the electrodes of a capacitor, C_0 is the capacitance of a capacitor layer between two electrodes, and L is the thickness of an element layer. The coefficient α is donated as the rate of change of the capacitance with the thickness. Equation (1) is the mathematical foundation of many vibration models of power capacitors such as the black-box model and the frequency domain finite element model. A black-box model was used to predict the sound pressure level of power capacitors. The black-box model consisted of several transfer functions used to describe the relation between the voltage applied on a capacitor and the vibration on surfaces [6–8] but the vibration inside the capacitor core could not be not provided. The transfer function method is used under the assumption of a linear time-invariant system, which may not be exact for a power capacitor. For the vibration inside a capacitor, numerical finite element models are usually employed in the frequency domain. Electric forces derived from the voltage on a capacitor, as shown in Equation (1), were input into a finite element model to calculate the corresponding mechanical vibration [10]. The calculation was conducted in the frequency domain. In the result, the frequency of vibration was definitely equal to that of the electric force, which was not fully consistent with the experimental observations [11,12].

In previous studies, it has been supposed that the coefficient α was time-independent for a specific power capacitor and the frequencies of the mechanical vibration and acoustic noise were consistent with the frequency of the electric force. However, the coupling effect between the mechanical vibration and the electric force was not accommodated in the previous models. On one hand, the electric force was the excitation of the mechanical vibration; on the other hand, the mechanical vibration made the coefficient α change with time and affected the electric force. The electro-mechanical coupling had a significant effect on the frequency response of the capacitor vibration. Therefore, a new vibration model of a power capacitor core is proposed in this paper. This vibration model took into account the coupling between the electric force and the mechanical vibration and implied new features; for example, that the frequency of vibration was not equal to that of the electric force.

A vibration model of a power capacitor core with an electro-mechanical coupling was built; the mathematical equations derived are shown in Section 2. According to the vibration model, new features corresponding with the electro-mechanical coupling were analyzed such as the frequency spectrum of the vibration (Section 3). As shown in Section 4, the vibration of the capacitor cores was measured and the theoretical features derived from the electro-mechanical coupling were observed in the experiment.

2. Vibration Model of a Power Capacitor Core

The power capacitor consisted of a stainless steel case, two bushings, and internal capacitor elements. The capacitor element was composed of two aluminum foils as electrodes and polypropylene films as insulations, which were wound and flattened into a rectangular shape. From a larger view of the capacitor elements, it could be considered to be a numerous plate capacitor in a series, as shown in Figure 1.

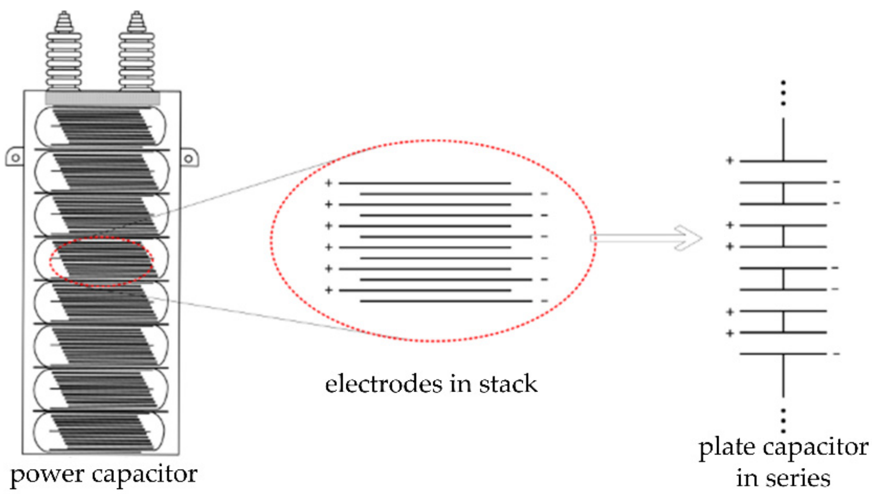

Figure 1. Diagram of a capacitor core.

In the above structure, the distance between the aluminum foil plates of the capacitor, which was 20~30 μm [13], was much smaller than the length of the core. The overall length of a capacitor core is generally larger than 0.5 m composed of a large number of parallel stacked electrode plates. Therefore, it can be modeled and analyzed as a continuous structure with infinite degrees of freedom.

Based on the theory of continuum mechanics, a vibration model of a power capacitor was established in this paper. In elasticity, an elastic body is a spatially continuous structure and there are compression and shear interactions between its internal materials. However, differing from general elastic continuous structures, there are electric forces between the electrodes in power capacitors that are related not only to the voltage applied but also to the distance between the aluminum plates. When a capacitor plate vibrates, the distance between the plates simultaneously changes, which has an impact on the electric forces. Meanwhile, the electric forces actuate the capacitor plate to vibrate. Therefore, the electric force and mechanical vibration of the power capacitor are coupled. Thus, the coupling effects of the electric field and mechanical vibration should be considered at the same time in a vibration model.

In this paper, the principle of least action was used to model the vibration of a capacitor core. The form of the vibration model and the corresponding reference coordinate system are shown in Figure 2.

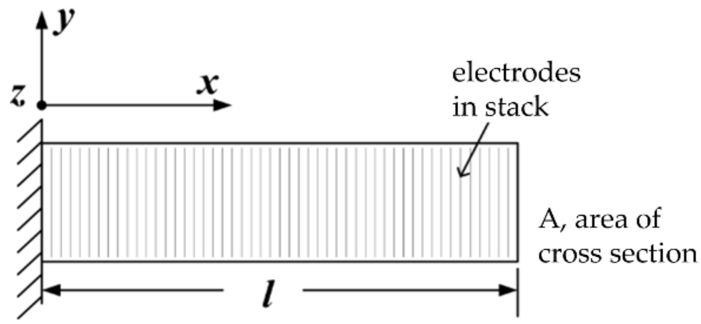

Figure 2. Diagram of vibration model of power capacitor core.

The origin of the reference coordinate system was set at the centroid of the capacitor core. The length of the core was in the x-axis direction and the cross-section was parallel to the yOz plane. Under electrical excitation, the electric forces interacted between the electrode plates, which were the internal forces in the system. According to the theorem of centroid motion, the position of the centroid located on the cross-section at half of the length does not change with time, which is equivalent to a fixed constraint. The dielectric materials (polypropylene film and capacitor oil) between the two electrodes were regarded as equally belonging to the two electrodes on both sides; a layer of an electrode together with its attached dielectric could then be used as a micro-element of the elastic continuum. The number of micro-elements was infinite and the vibration model of the filter capacitor core could be described by partial differential equations.

When the mechanical vibration was excited by the electric force in the power capacitor, the total action of this capacitor system was the sum of the electrical action and the mechanical action, as below:

$$S = \int_{t_1}^{t_2} \int_0^l [\frac{1}{2}\rho A\left(\frac{\partial \xi}{\partial t}\right)^2 - \frac{1}{2}EA\left(\frac{\partial \xi}{\partial x}\right)^2 + \frac{1}{2}C_0(\xi, t)u^2(t)]\mathrm{d}x\mathrm{d}t \quad (2)$$

where S is the total action of the capacitor system, ρ is the mass density of the capacitor core, ξ is the displacement of the micro-element, E is the elastic modulus of the capacitor core, C_0 is the capacitance of a capacitor layer between two electrodes, and $u(t)$ is the voltage applied on the capacitor. The first term in the above integral formula was the kinetic energy density of the capacitor in space. The second was the density of the elastic potential energy.

The third was the electrical potential energy of a single layer capacitor, which could be expressed as:

$$\begin{aligned} E_C^{(0)} &= \frac{1}{2}C_0(\xi,t)u^2(t) = \frac{1}{2}\frac{\varepsilon A}{d_0(1+\frac{\partial\xi}{\partial x})}u^2(t) \\ &\approx \frac{1}{2}\frac{\varepsilon A}{d_0}u^2(t) - \frac{1}{2}\frac{\varepsilon A}{d_0^2}\frac{\partial\xi}{\partial x}u^2(t) + \frac{1}{2}\frac{\varepsilon A}{d_0^3}\left(\frac{\partial\xi}{\partial x}\right)^2 u^2(t) \end{aligned} \tag{3}$$

where $E_C^{(0)}$ is the electrical potential energy of a single layer capacitor, ε is the dielectric constant of the capacitor, and d_0 is the distance between two electrodes under no electrical excitations. This electrical potential energy was retained up to a second-order term of polynomials to maintain the same order as the elastic potential energy.

Substituting Equation (3) into Equation (2), and conducting a variation of the total action of the system, it was obtained that:

$$\begin{aligned} \delta S &= A\int_{t_1}^{t_2}\int_0^l [\rho\frac{\partial\xi}{\partial t}\delta\frac{\partial\xi}{\partial t} - E\frac{\partial\xi}{\partial x}\delta\frac{\partial\xi}{\partial x}]\mathrm{d}x\mathrm{d}t \\ &\quad -A\int_{t_1}^{t_2}\int_0^l [\frac{1}{2}\frac{\varepsilon}{d_0^2}u^2(t)\delta\frac{\partial\xi}{\partial x} - \frac{\varepsilon}{d_0^3}\frac{\partial\xi}{\partial x}u^2(t)\delta\frac{\partial\xi}{\partial x}]\mathrm{d}x\mathrm{d}t \\ &= A\int_{t_1}^{t_2}\int_0^l [-\rho\frac{\partial^2\xi}{\partial t^2} + (E - \frac{\varepsilon}{d_0^3}u^2(t))\frac{\partial^2\xi}{\partial x^2}]\delta\xi\mathrm{d}x\mathrm{d}t \\ &\quad -A\int_{t_1}^{t_2} [(E - \frac{\varepsilon}{d_0^3}u^2(t))\frac{\partial\xi(l,t)}{\partial x} + \frac{1}{2}\frac{\varepsilon}{d_0^2}u^2(t)]\delta\xi(l,t)\mathrm{d}t \end{aligned} \tag{4}$$

Given that δS = 0, based on the principle of least actions, the multiplying terms of $\delta\xi$ and $\delta\xi(l,t)$ were equal to zero in Equation (4). Thus, a differential equation along with the boundary conditions was derived, which represented the mechanical vibration of the power capacitor core as:

$$\begin{cases} \rho\frac{\partial^2\xi}{\partial t^2} = (E - \frac{\varepsilon}{d_0^3}u^2(t))\frac{\partial^2\xi}{\partial x^2} \\ \xi(0,t) = 0 \\ (E - \frac{\varepsilon}{d_0^3}u^2(t))\frac{\partial\xi(l,t)}{\partial x} = -\frac{1}{2}\frac{\varepsilon}{d_0^2}u^2(t) \end{cases} \tag{5}$$

The right hand side of the partial differential equation demonstrates that there was a coupling between the mechanical vibration and the electric field of the capacitor core, which could be regarded as a time-dependent elastic modulus of the capacitor core structure. This coupling could generate the capacitor to produce more high-frequency components of the mechanical vibration and cause the frequency spectrum to become more complex.

3. Theoretical Analysis of the Frequency Response of the Capacitor Vibration

According to the vibration model of the capacitor core, the mechanism of multi-frequency vibration was analyzed via solving the vibration equation. In order to obtain the solution, a perturbation method was used to deal with the coupling term of the equation.

Given that $\mu = \varepsilon U^2/(2{d_0}^3 E)$ as the dimensionless parameter that characterized the effect of the coupling between the vibration and the electric field, and that $\nu = -\varepsilon U^2/(4{d_0}^2 E)$ to characterize the degree of electrical excitation, the vibration equation turned to:

$$\begin{cases} \frac{\partial^2\xi}{\partial t^2} = c^2[1 - \mu(1+\cos\omega_E t)]\frac{\partial^2\xi}{\partial x^2} \\ \xi(0,t) = 0 \\ [1 - \mu(1+\cos\omega_E t)]\frac{\partial\xi(l,t)}{\partial x} = v(1+\cos\omega_E t) \end{cases} \tag{6}$$

where c is the speed of the vibration wave and ω_E is the angular frequency of the electric force, which had a relation with the angular frequency of the voltage ω as $\omega_\mathrm{E} = 2\omega$ when the capacitor was applied to a sinusoidal voltage.

According to the perturbation method, the vibrational displacement of a capacitor core can be expressed as:

$$\xi(x,t;\mu) = \xi_0(x,t) + \mu\xi_1(x,t) + \mu^2\xi_2(x,t) + \ldots \tag{7}$$

where $\xi(x,t;\mu)$ is the displacement of the capacitor core at position x and μ determines the form of ξ functions. $\xi_0(x,t)$ is the presumptive solution when neglecting the coupling effect, i.e., $\mu = 0$. $\xi_i(x,t)$, where $i = 1, 2, 3, \ldots$, are corrective solutions to supplement the $(i-1)$ solutions stated before.

Substituting Equation (7) to Equation (6), it was obtained that:

$$\begin{cases} \frac{\partial^2\xi_0}{\partial t^2} + \mu\frac{\partial^2\xi_1}{\partial t^2} + \mu^2\frac{\partial^2\xi_2}{\partial t^2} + \ldots = c^2[1-\mu(1+\cos\omega_E t)](\frac{\partial^2\xi_0}{\partial x^2} + \mu\frac{\partial^2\xi_1}{\partial x^2} + \mu^2\frac{\partial^2\xi_2}{\partial x^2} + \ldots) \\ \xi_0(0,t) + \mu\xi_1(0,t) + \mu^2\xi_2(0,t) + \ldots = 0 \\ \left[1-\mu(1+\cos\omega_E t)\right](\frac{\partial\xi_0(l,t)}{\partial x} + \mu\frac{\partial\xi_1(l,t)}{\partial x} + \mu^2\frac{\partial\xi_2(l,t)}{\partial x} + \ldots) = v(1+\cos\omega_E t) \end{cases} \tag{8}$$

By setting the coefficients of the polynomial of μ to be zero, a series of partial differential equations was obtained; e.g., for the μ^0 term, the corresponding equations were:

$$\begin{cases} \frac{\partial^2\xi_0}{\partial t^2} = c^2\frac{\partial^2\xi_0}{\partial x^2} \\ \xi_0(0,t) = 0 \\ \frac{\partial\xi_0(l,t)}{\partial x} = v(1+\cos\omega_E t) \end{cases} \tag{9}$$

and the stationary solution of Equation (9) was:

$$\xi_0(x,t) = v\left(\frac{1}{k\cos kl}\sin kx\cos\omega_E t + x\right) \tag{10}$$

where k was the wave number of the mechanical vibration and $k = \omega_E/c$. Equation (9) was the presumptive solution when neglecting the coupling effect and this vibration had the same angular frequency ω_E with the electric force on the capacitors. When the electric force angular frequency ω_E approached the natural frequency of the capacitor structure, i.e., $\cos(kl) = 0$, Equation (10) became infinity and the power capacitor was in mechanical primary resonance with a series of natural frequencies as:

$$\omega_n = \frac{c}{l}(\frac{\pi}{2} + i\pi)\ i = 0,\ 1,\ 2,\ 3,\ \ldots. \tag{11}$$

For the μ^1 term, the corresponding equations were:

$$\begin{cases} \frac{\partial^2\xi_1}{\partial t^2} = c^2\frac{\partial^2\xi_1}{\partial x^2} - c^2(1+\cos\omega_E t)\frac{\partial^2\xi_0}{\partial x^2} \\ \xi_1(0,t) = 0 \\ \frac{\partial\xi_1(l,t)}{\partial x} = (1+\cos\omega_E t)\frac{\partial\xi_0(l,t)}{\partial x} \end{cases} \tag{12}$$

Substituting Equation (10) into Equation (12), the equation for the first-order corrective solution $\xi_1(x,t)$ was obtained as:

$$\begin{cases} \frac{\partial^2\xi_1}{\partial t^2} = c^2\frac{\partial^2\xi_1}{\partial x^2} + c^2 v\frac{k}{\cos kl}\sin kx(\frac{1}{2} + \cos\omega_E t + \frac{1}{2}\cos 2\omega_E t) \\ \xi_1(0,t) = 0 \\ \frac{\partial\xi_1(l,t)}{\partial x} = v(\frac{3}{2} + 2\cos\omega_E t + \frac{1}{2}\cos 2\omega_E t) \end{cases} \tag{13}$$

The effects of the coupling term in Equation (6) acted as the excitation term in Equation (13), having a constant component, a ω_E component, and a $2\omega_E$ component. Thus, the stationary solution of Equation (13) was:

$$\begin{aligned}\xi_1(x,t) &= \frac{v}{2}\frac{1}{\cos kl}\left(x\cos kx + \frac{kl\tan kl+1}{k}\right)\cos\omega_E t \\ &+\frac{v}{2}\left(-\frac{\sin kx}{3k\cos kl}+\frac{2\sin 2kx}{3k\cos 2kl}\right)\cos 2\omega_E t+\frac{v}{2}\left(\frac{\sin kx}{k\cos kl}+2x\right)\end{aligned} \tag{14}$$

From Equation (14), a clue of the new frequency component of the vibration could be observed. The first-order corrective solution had a frequency spectrum of ω_E and $2\omega_E$ components. In the same way, the Nth-order corrective solution had a component with the angular frequency $(N + 1)\omega_E$.

Substituting Equations (10) and (14) into Equation (7), the mechanical vibration of the capacitor core was:

$$\begin{aligned}\xi(x,t) &= v\{\,[\frac{\sin kx}{k\cos kl}+\frac{\mu}{2}(x\frac{\cos kx}{\cos kl}+\frac{kl\tan kl+1}{k}\frac{\sin kx}{\cos kl})+\ldots]\cos\omega_E t \\ &+[\frac{\mu}{2}(-\frac{\sin kx}{3k\cos kl}+\frac{2\sin 2kx}{3k\cos 2kl})+\ldots]\cos 2\omega_E t+(x+\mu x+\ldots)+\ldots\,\}\end{aligned} \tag{15}$$

It could be seen that the coupling between the mechanical vibration and the electric field caused a so-called multi-frequency vibration phenomenon. The frequencies of vibration were integer multiples of the frequency of the voltage applied on the capacitors. According to the theory of small oscillation [14], the vibration displacement of the capacitor core is a small amount relative to its structural size. According to Equation (15), in general, the multi-frequency components caused by coupling were higher level small quantities with respect to the parameter μ, making it difficult to measure the multi-frequency vibration on every capacitor. However, under the condition of resonance, the multi-frequency vibration became predominant.

The term of $\cos(2\omega_E t)$ in Equation (15) was expressed as:

$$\begin{aligned}\xi^{(2\omega_E)} &= v\frac{\mu}{2}\left(-\frac{\sin kx}{3k\cos kl}+\frac{2\sin 2kx}{3k\cos 2kl}\right)\cos 2\omega_E t \\ &= v\frac{\mu}{2}\left[-\frac{\sin kx}{3k\cos(\frac{\omega_E}{c}l)}+\frac{2\sin 2kx}{3k\cos(2\frac{\omega_E}{c}l)}\right]\cos 2\omega_E t\end{aligned} \tag{16}$$

When $\cos(2kl) = 0$, the $2\omega_E$ component moved the level of μ^1 to the level of μ^0. This status is named the superharmonic resonance in mechanics, having a frequency of excitation equal to 0.5 times the natural frequency [15]. For the capacitors, the relation was expressed as:

$$\omega_E = \frac{(2n-1)\pi}{4}\frac{c}{l} = \frac{\omega_n}{2} \tag{17}$$

Therefore, Equation (17) was the trigger of the predominant multi-frequency vibration on the power capacitor. At this status, the power capacitor structure was in superharmonic resonance.

4. Measurement of the Capacitor Vibration

Firstly, the vibration on a capacitor unit was measured to verify the above vibration model of the power capacitor core. The experimental setup is shown in Figure 3. A harmonic source was utilized to generate a sinusoidal voltage with a frequency ranging from 50 Hz~1500 Hz and an amplitude of 0 V~350 V. As the voltage amplitude was too low for the power capacitors, a transformer, equipped with an amorphous alloy core with less loss at a high frequency, was used to extend the voltage range to 0 V~12 kV. The capacitor unit, with ratings of 8.15 kV and 8.9 μF, was subjected to a 550 Hz 690 V sinusoidal voltage. Limited by the capacity of the source, a high-voltage reactor was employed as compensation. The reactor was adjusted to form a parallel circuit with the capacitor at 550 Hz. In the test, the vibration velocity on the bottom surface of the capacitor was measured by a laser Doppler vibrometer (Ploytec, Baden-Württemberg, Germany).

As a 550 Hz sinusoidal voltage was applied to the capacitor, the frequency of vibration could be derived according to previous studies [1,6,7]. Substituting:

$$u(t) = U\cos(2\pi\cdot 550\cdot t)$$

into Equation (1):

$$F_e = \alpha U^2\cos^2(2\pi\cdot 550\cdot t) = \frac{\alpha U^2}{2} + \frac{\alpha U^2}{2}\cos(2\pi\cdot 1100\cdot t) \quad (18)$$

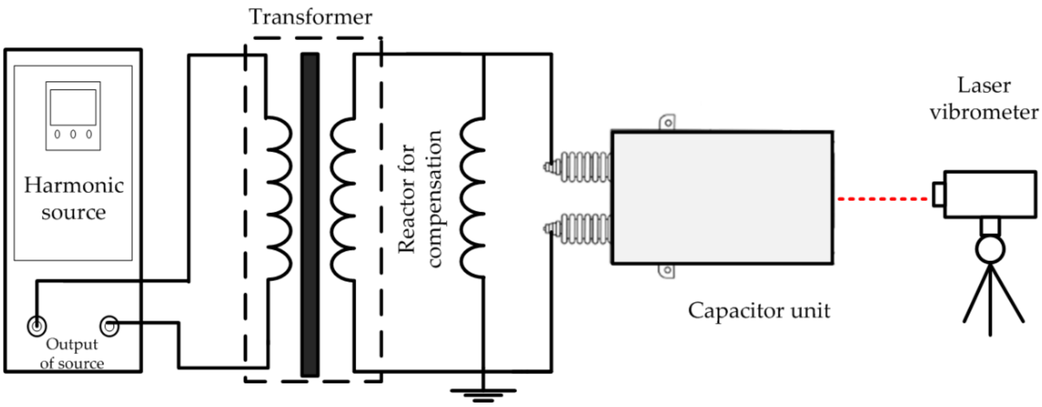

Figure 3. Experimental setup for vibration measurement of a capacitor unit.

Thus, the vibration spectrum should be 1100 Hz if the electro-mechanical coupling was not considered, which is the method used by most previous studies. The frequency spectrum of the vibration velocity of the capacitor in the test is demonstrated in Figure 4. Although the voltage on the excitation of the capacitor was at the frequency of 550 Hz, the corresponding vibration had frequencies that were integer multiples of that of voltage. The result was consistent with the multi-frequency characteristic derived in the vibration model.

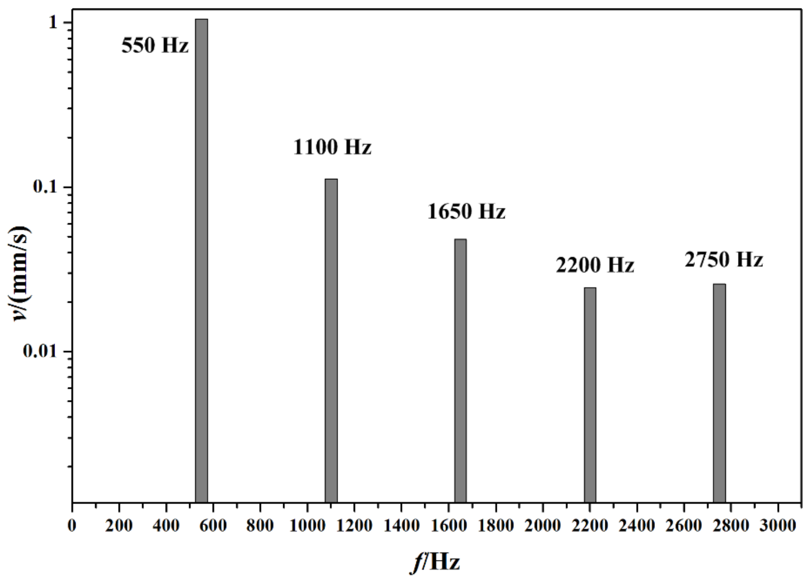

Figure 4. Vibration velocity on the bottom surface of a capacitor unit under 550 Hz 690 V sinusoidal voltage excitation.

The frequency response of the vibration under an electrical excitation was measured. Limited by the frequency and amplitude imposed by the harmonic power supply, a capacitor core without oil impregnation was employed. The capacitor core was a stack of 20 elements with a capacitance of 22 μF, as shown in Figure 5.

The experimental setup consisted of a harmonic source, a transformer, and a laser Doppler vibrometer, as shown in Figure 6. In the test, a series of sinusoidal voltages with different frequencies was applied to the core so no reactors were used as a parallel compensation. The vibration velocity as a response at the end of the core was measured by a laser Doppler vibrometer under voltages with different frequencies.

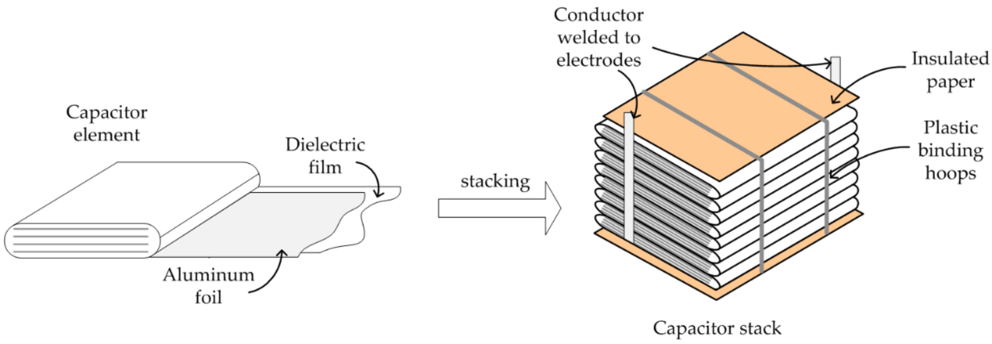

Figure 5. Capacitor core without oil impregnation.

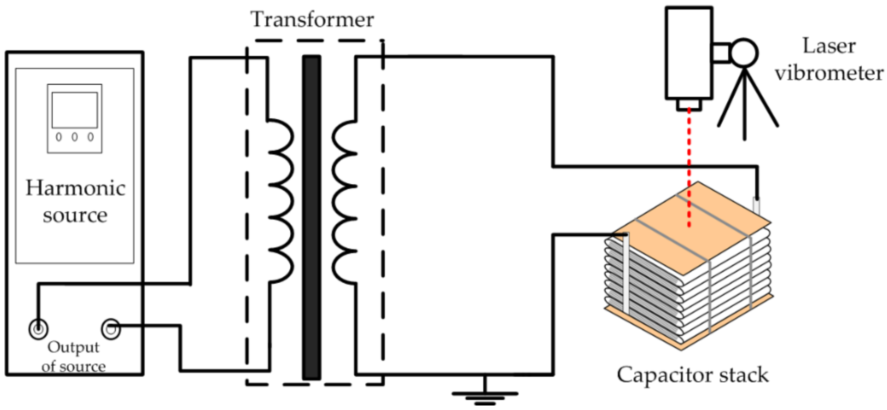

Figure 6. Experimental setup for capacitor stack vibration measurement (no reactor for compensation).

By gradually changing the frequency of the excitation voltage, the response curve of the mechanical vibration with the frequency of the voltage squared could be drawn, as shown in Figure 7. According to the vibration model, the theoretical frequency response of the vibration velocity (shown in Figure 8) was calculated by:

$$H_v(\omega_E) = \frac{1}{4}\frac{\varepsilon U^2}{d_0^2\sqrt{E\rho}}\tan kl = \frac{1}{4}\frac{\varepsilon U^2}{d_0^2\sqrt{E\rho}}\tan\left(\frac{\pi}{2}\frac{\omega_E}{\omega_n{}^{(1)}}\right) \quad (19)$$

where $\omega_n{}^{(1)}$ is the first-order natural frequency of the capacitor core given by Equation (11) with $i = 0$.

A series of peak points could be observed in the frequency response curve, as seen in Figure 7, and the corresponding frequencies were the structural natural frequency of the capacitor core. The frequency interval between each natural frequency was equal and there was an anti-resonance point with a small response between two adjacent natural frequencies. The above natural frequency distribution was consistent with Equations (10) and (11) derived from the vibration model. Compared with Figure 8, the amplitude of the frequency response was different from the model. For the actual capacitor, a certain damping effect existed due to friction and the vibration response could not reach infinity as deduced by the model. This damping effect strengthened with the increase in the frequency, making the response amplitude smaller, which was also consistent with the results measured, as shown in Figure 7.

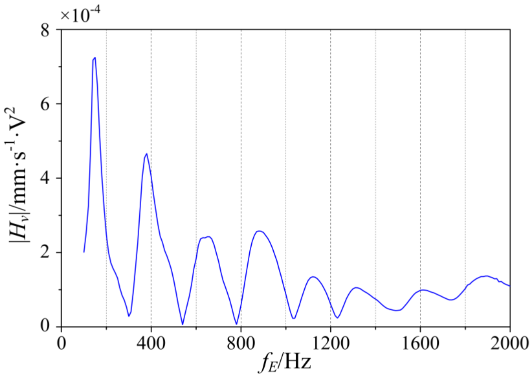

Figure 7. Frequency response of core vibration.

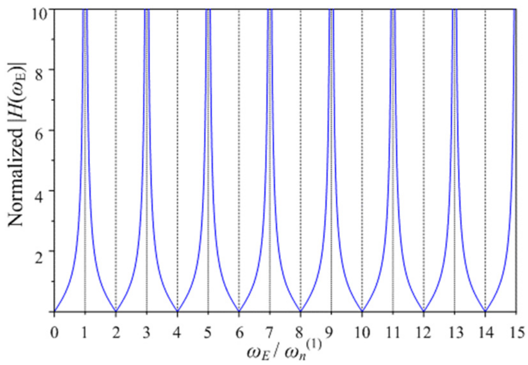

Figure 8. Frequency response of core vibration calculated by the theoretical model (first-order natural frequency $\omega_n^{(1)}$ was used as normalization to describe the frequency on horizontal axis).

In order to continue to investigate the multi-frequency vibration, the vibration of the capacitor core in the actual power capacitor was measured. The capacitor adopted had a rated voltage of 8.9 kV, a rated current of 30.15 A, and a nominal capacitance of 10.786 µF. The length of the core was 670 mm and the section size was 355 mm. The capacitor cores were impregnated with oil and encapsulated in stainless steel. In order to approach the actual state of the core as closely as possible, the core was kept in the impregnated state in oil during the test measurement. The top cover of the capacitor was cut off, the capacitor was kept vertical, and a small amount of oil was extracted from the top so that a part of the end of the capacitor core was exposed for measuring its vibration. The rest remained immersed in the oil.

In the test, the vibration of the oil-immersed core was measured from the vertical direction by a laser Doppler vibrometer. Sinusoidal voltages with different frequencies were applied, starting from 50 Hz to 1000 Hz with an interval of 5 Hz. The frequency of the electric field force started at 100 Hz, the frequency interval was 10 Hz, and the ending frequency was 2000 Hz. The vibration velocity component of the capacitor equal to the frequency of the electric force was measured and its frequency response curve was obtained, as shown in Figure 9.

As can be seen from Figure 6, in the frequency range of 100 Hz~2000 Hz, there was only the first natural frequency, which was 1180 Hz. Compared with the frequency response curve of the dry core in Figure 7, the natural frequency of the oil-immersed core became higher. This was because the layers of the dry core were filled with air; the internal air was squeezed out when the element was compressed whereas the layers in the oil-immersed core were filled with capacitor oil. The oil gaps between the layers were about 30 µm, which was too small for the viscous oil to flow. This led to a stiffness of the oil-immersed core greater than that of the dry core and its natural frequency increased accordingly. For the core vibration model of the power capacitor, there was still a second-order natural frequency of 3540 Hz in the higher frequency band.

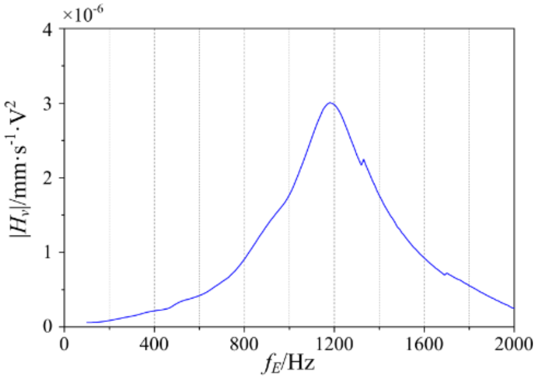

Figure 9. Frequency response function of vibration of a capacitor core immersed in oil (vibration components consistent with electric force frequency were extracted).

The coupling between the electric field and the mechanical vibration of the oil-immersed core was further investigated. The component with its frequency equal to two times of that of the electric force in the vibration was extracted; the frequency response function curve is shown in Figure 10.

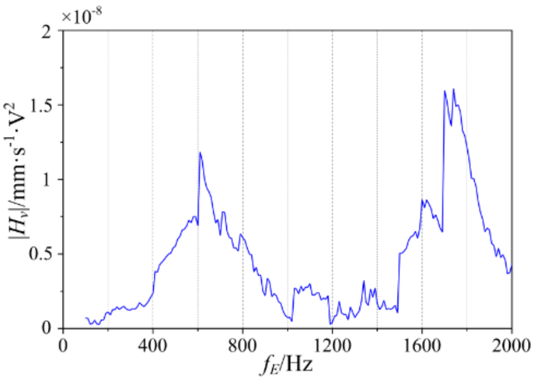

Figure 10. Frequency response function of oil core vibration of a capacitor (vibration components with doubled electric force frequency were extracted).

In Figure 10, when the frequency of the electric force was close to 0.5 times of the measured natural frequency of 1180 Hz, a significant peak appeared in the vibration frequency response curve, indicating that the superharmonic resonance was excited. In addition, for the second-order natural frequency of 3540 Hz, there was also a peak in the frequency response curve near to 0.5 times the frequency. This verified that the vibration model was also applicable to an oil-immersed capacitor core.

5. Conclusions

In this paper, the multi-frequency vibrations of power capacitor cores were analyzed by constructing a vibration model of a capacitor core. The following conclusions were obtained:

(1) The physical basis of the multi-frequency vibration of the power capacitors was the coupling between the electric force and the mechanical vibration, which made the vibration equation of the capacitor behave as a variable coefficient differential equation;
(2) The power capacitor had multiple natural frequencies and the frequency difference between two adjacent natural frequency points was the same;
(3) When the frequency of the electric force was close to 0.5 times the natural frequency, it triggered the capacitor to produce a predominant multi-frequency vibration and the electric force at this frequency excited the superharmonic resonance of the power capacitor.

Author Contributions: Conceptualization, J.L.; methodology, J.L.; validation, J.L., X.L. and Z.Z.; formal analysis, J.L. and Y.X.; investigation, J.L.; resources, Y.X.; data curation, X.L.; writing—original draft preparation, J.L.; writing—review and editing, X.L.; visualization, J.L.; supervision, Y.X.; project administration, J.L.; funding acquisition, J.L. All authors have read and agreed to the published version of the manuscript.

Funding: This research was funded by the China Electric Power Research Institute with project "Investigation on the electrodynamics behavior of electro-induced vibration", grant number "5242001900DQ".

Institutional Review Board Statement: The study did not require ethical approval.

Informed Consent Statement: The study did not involve humans.

Data Availability Statement: The data presented in this study are available on request from the corresponding author upon reasonable request.

Conflicts of Interest: The authors declare no conflict of interest. The funders had no role in the design of the study; in the collection, analyses, or interpretation of data; in the writing of the manuscript, or in the decision to publish the results.

Abbreviations

α	Rate of change of capacitance with thickness
C_0	Capacitance of a capacitor layer between two electrodes
c	Speed of the vibration wave in a capacitor core
d_0	Distance between two electrodes under no electrical excitations
E	Elastic modulus of a capacitor core
$E_C^{(0)}$	Electric potential energy of a single layer capacitor
ε	Dielectric constant of the dielectrics in a capacitor
F_e	Electric force acting on the electrodes of a capacitor
k	Wave number of vibrations in a capacitor core
ξ	The displacement of micro-elements in a capacitor core
$\xi_0(x,t)$	Presumptive solution of displacement of micro-elements when neglecting the coupling effect
$\xi_i(x,t)$	The ith corrective solution of the displacement of micro-elements
L	The thickness of an element layer
l	Half of the length of a capacitor core
ρ	Mass density of a capacitor core
S	Total action of a capacitor system
μ	Dimensionless parameter to characterize the coupling between the vibration and electric field, which is $\mu = \varepsilon u^2/(2{d_0}^3 e)$
$u(t)$	Voltage applied on a capacitor
ν	Dimensionless parameter to characterize the degree of electrical excitation, which is $\nu = -\varepsilon u^2/(4{d_0}^2 e)$
ω	Angular frequency of a voltage applied to a capacitor
ω_E	Angular frequency of the electric force
ω_n	Natural frequency of a capacitor core in radian units
${\omega_n}^{(1)}$	First-order natural frequency of a capacitor core in radian units

References

1. Roget, A.B. Study of Vibration and Audible Noise Generated by Shunt Capacitor Banks at Substations Serving Non-Linear Loads. Doctoral Dissertation, University of Alabama, Tuscaloosa, AL, USA, 2011.
2. McDuff, G. Electrical power losses due to acoustic wave generation in repetitive pulsed capacitors. In Proceedings of the IEEE Conference Record of the 1988 Eighteenth, Hilton Head, SC, USA, 20–22 June 1988.
3. Cox, M.D.; Guan, H.H. Vibration and audible noise of capacitors subjected to nonsinusoidal waveforms. *IEEE Trans. Power Deliv.* **1994**, *9*, 856–862. [CrossRef]
4. International Electrotechnical Commission. *IEC/TS 61973 High Voltage Direct Current (HVDC) Substation Audible Noise*; IEC: Geneva, Switzerland, 2012.
5. Clark, M.; Grisenti, A.; Jensen, C.; Kataoh, A.; Lubini, E.; Nyman, A.; Eidhin, G.; Reschner, W.; Samuelsson, H. *HVDC Station Audible Noise*; CIGRE Technical Report: Paris, France, 2002.

6. Ji, S.; Wu, P.; Zhang, Q.; Li, Y. Study on the Noise-Level Calculation Method for Capacitor Stacks in HVDC Converter Station. *IEEE Trans. Power Deliv.* **2010**, *25*, 1866–1873.
7. Zhu, L.; Ji, S.; Shen, Q.; Liu, Y.; Li, J.; Liu, H. A noise level prediction method based on electro-mechanical frequency response function for capacitors. *PLoS ONE* **2013**, *8*, e81651. [CrossRef] [PubMed]
8. Bandalo, F.S.; Singh, B.; Sévigny, R. Audible Noise and High-Voltage Power Capacitors. *IEEE Trans. Power Deliv.* **2018**, *33*, 2437–2441. [CrossRef]
9. Li, J.; Ji, S.; Zhu, L.; Wu, P.; Cao, T. Vibration Characteristics of Filter Capacitors Used in HVDC Converter Stations. *IEEE Trans. Power Deliv.* **2017**, *32*, 2263–2271. [CrossRef]
10. Kim, H.; Kim, D.; Park, N.; Park, Y. Acoustic noise and vibration analysis of solid state drive induced by multi-layer ceramic capacitors. *Microelectron. Reliab.* **2018**, *83*, 136–145. [CrossRef]
11. Shi, Y.; Ji, S.; Zhang, F.; Ren, F.; Zhu, L.; Lv, L. Multi-Frequency Acoustic Signal Under Short-Circuit Transient and Its Application on the Condition Monitoring of Transformer Winding. *IEEE Trans. Power Deliv.* **2019**, *34*, 1666–1673. [CrossRef]
12. Li, J.; Zhu, L.; Xiong, Y.; Lei, X.; Ji, S. Mechanism model of multi-times-frequency spectrum of filter capacitor vibration and audible noise. *High Voltage Eng.* **2018**, *44*, 2081–2088.
13. Natarajan, R. *Power System Capacitors*; CRC Press: Boca Raton, FL, USA, 2005.
14. Landau, L.D.; Lifshitz, E.M. *Mechanics, Volume 1 of Course of Theoretical Physics*, 3rd ed.; Pergamon Press: New York, NY, USA, 2000; pp. 80–84.
15. Morse, P.; Feshbach, H. *Methods of Theoretical Physics*; McGraw-Hill: New York, NY, USA, 1953; pp. 523–576.